Effect of Joint Misalignment in Upper Limb Exoskeleton Based on McKibben Muscles

Effect of joint misalignment in upper limb exoskeleton based on McKibben muscles

Maria Paterna[0000-0001-5484-7491], **Carlo De Benedictis***[0000-0003-0687-0739] **and Carlo Ferraresi**[0000-0002-9703-9395]

Department of Mechanical and Aerospace Engineering, Politecnico di Torino, Turin, Italy
carlo.debenedictis@polito.it

Abstract One of the critical issues in the design of an exoskeleton is the matching between exoskeleton's and human's kinematic chains. The misalignments between the exoskeleton and human joints' rotation axes may reduce the support action provided by an exoskeleton or introduce shear forces on the human limbs at the attachment points of the exoskeleton. This paper aims to assess the effect of misalignments in the design of a custom industrial upper limb passive exoskeleton based on McKibben's muscles.

Keywords Joint Misalignment, Upper Limb Exoskeleton, Passive Exoskeleton, Pneumatic Artificial Muscles, McKibben.

1 Introduction

Upper limb exoskeletons are passive or active devices that often imitate human kinematics to assist upper limb motions and empower the user. The upper limb can be considered to have nine degrees of freedom (DoF): five DoFs at the shoulder, two DoFs at the elbow, and two DoFs at the wrist. Shoulder DoFs consist of humerus flexion/extension, abduction/adduction, internal/external rotation, and translation of the shoulder joint center (SJC) on the frontal plane; elbow DoFs consist of forearm flexion/extension and prono/supination; wrist DoFs consist of hand flexion/extension and abduction/adduction.

Misalignment between the exoskeleton and shoulder joints axes could reduce the working range and cause discomfort, pain, and in severe cases lead to dislocation and fractures [1, 2]. Different strategies have been implemented to avoid this issue. Some studies attempted to replicate human joint kinematics: for instance, H-Vex [3] employs a four-bar polycentric construction to track the shoulder joint

movement in the transverse plane and prevent the rotational axes of the exoskeleton joint and the shoulder joint from being misaligned. On the other hand, Liu et al. [4] employed a back support shaft that can rotate on the frontal plane to allow the exoskeleton shoulder joint to follow the elevation and depression of the wearer's shoulder complex. However, achieving complete human-exoskeleton kinematic compatibility remains hard due to intersubject variability and the difficulty of precisely locating the human joint axes. Therefore, other studies tried to explicitly follow the kinematic of the limb without copying its structure. To this aim, highly redundant exoskeletons have been constructed to improve the fit between the robotic device and the human limb [5]. For example, the MATE [6] flexion/extension axis aligns with the anatomical one. However, there is no alignment between the hinge that generates the abduction/adduction and the physiological axis. The hinge is combined with a horizontal slider so as not to interfere with the normal range of motion of the human arm. N-bar linkage mechanism [7−9] or parallel rotational joints in series [10] are also used to compensate misalignments. On the other hand, the design process used in PAEXO is unique [11]. There is only one hinge, with a fixed axis of rotation, that joins the arm bar and support bar. Even though the exoskeleton kinematic chain does not mimic a human joint, the user has a wide range of motion and multiple degrees of freedom because of the implementation of ball joints between the bars and the human-exoskeleton interface, as well as due to the absence of stiff components behind the back.

In previous works from the authors [12, 13], McKibben artificial muscles (MKMs) have been selected as elements for energy storage and torque generation in a passive exoskeleton for overhead work support. In particular, commercial MKMs (DMSP-10-350N-RM-CM, FESTO, Germany) have been implemented in a custom exoskeleton design based on a *shoulder pad* integrated into the mechanical structure, which has been conceived to match the torque provided by the device to the one requested to the anatomical joint during elevation of the arm. In such design, the force exerted by each MKM is transmitted via a Dyneema® wire (Braided climax - 200daN, OCKERT, Germany), whose direction is kinematically constrained by the shoulder pad, to a bracelet that supports the arm of the user. The exoskeleton has 2 DoFs and allows flex-extension and abd-adduction of the shoulder. Details of the exoskeleton architecture are provided in [12, 13] and are not presented in the current paper for the sake of conciseness. However, it should be highlighted that the performance of the proposed design is dependent on how well the exoskeleton joints axes fit the anatomical ones.

The main goal of this work is to evaluate and discuss the effects of joint misalignment in the exoskeleton design proposed by the authors in previous works [12, 13]. This problem has been tackled by modeling and simulation approaches. The degradation of performance due to misalignments is highlighted, as well as the magnitude of shear forces at the bracelet, transmitted to the human arm, that rise in such conditions. In this way, it should be possible to perform a more realistic assessment of the system behavior with respect to the theoretical one that considers perfect alignment between artificial and anatomical axes.

2 Joint misalignment issue

A kinematic chain with just two revolute degrees of freedom has been created to keep the exoskeleton structure compact and uncomplicated (Fig. 1). The first one is provided by a hinge that ensures shoulder flexion between 90° and 135° by positioning its horizontal axis in line with the shoulder flexion-extension axis. In order to allow horizontal plane abduction between 0° and 30°, the other is a vertical hinge axis that is in line with the shoulder abduction axis. Within the working range taken into consideration, the SJC moves approximately 2.8 cm upwardly and 0.3 cm medially [14]. The abduction-adduction joint misalignment may be disregarded because of the minimal displacement in the mediolateral direction. The impact of the misalignment between the flexion-extension joint center of the exoskeleton and the SJC in the sagittal plane is thus the main topic of this work.

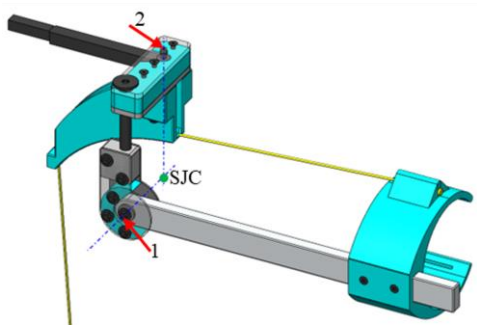

Fig.1 Design of the kinematic chain consisting of horizontal hinge axis (1) and vertical hinge axis (2). The green dot is the rotation axis intersection which should be aligned with SJC.

Assuming that the exoskeleton frame is rigidly fixed to the user trunk, the arm-bracelet connection is compliant, the bracelet must move along the upper arm by an amount d to permit shoulder flexion due to the SJC upward movement. This scenario is modeled as a statical mechanical issue in Fig. 2. The displacement amplitude d can be derived through geometric considerations (Eqs. (1)-(2)).

$$\left(-\Delta y-\frac{l}{\tan\theta_1}\right)\tan^2\frac{\beta}{2}+2l\tan\frac{\beta}{2}-\Delta y-\frac{l}{\tan\theta_1}=0 \tag{1}$$

$$l_v=\frac{l\cos\beta}{\sin\theta_1},\qquad d=l-l_v \tag{2}$$

In previous equations, l is the exoskeleton link length that is the distance between the bracelet and ExoJC (l=0.25 m); θ_1 is the shoulder elevation angle; Δy is the offset between SJC and ExoJC and can be computed thanks to the shoulder model

presented in [14] knowing the SJC-ExoJC relative position when θ_1=90°; β is the angle between the exoskeleton link and the horizontal axis; l_v is the distance between SJC and the bracelet.

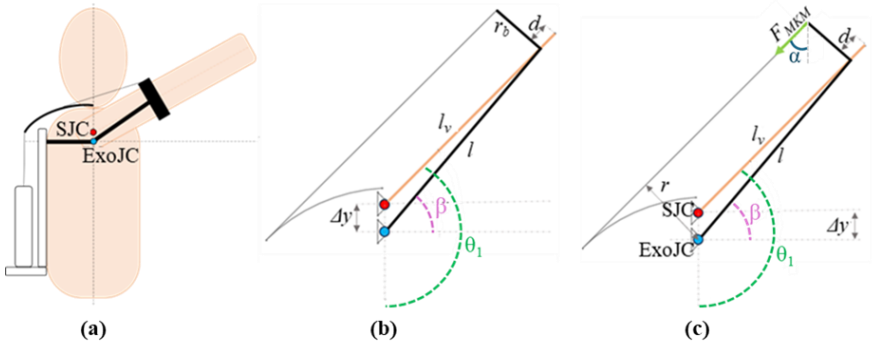

Fig.2 Joint misalignments between the exoskeleton and human limb (a). Diagrams for assessing the magnitude of bracelet displacement d (b) and the exoskeleton support torque (c).

The SJC-ExoJC misalignments and the consequent bracelet translation degrade the exoskeleton performance and, at the same time, cause the onset of a shear force on the user's arm. As Δy increases, the support torque provided by the exoskeleton (τ_{MKM}), expressed by Eqs. (3)-(4), decreases due to the reduction of the MKM traction force lever arm.

$$\tau_{MKM} = F_{MKM}\left(\sin\alpha\left(-l_v\cos\theta_1 + r_b\cos\beta\right) - \cos\alpha\left(l_v\sin\theta_1 - r_b\sin\beta\right)\right) \tag{3}$$

$$\alpha = \sin^{-1}\frac{r}{\sqrt{l^2 + r_b{}^2}} + \sin^{-1}\frac{l}{\sqrt{l^2 + r_b{}^2}} - \beta \tag{4}$$

On the other hand, the shear force (F_d) on the user's arm can be calculated by imposing a human-exoskeleton interface model. Soft tissues can be thought of as viscoelastic elements from a mechanical perspective, meaning that the induced force is proportionate to the deformation and rate of deformation. They must take into account both the nature of the soft tissue and the material that makes up the exoskeleton bracelet to evaluate the shear force F_d that is applied to the arm using Eq. (5), where k_{arm} and c_{arm} stand for the stiffness and damping coefficients of the human-exo contact surface. According to the literature [5], the shear force F_d is computed under quasi-static conditions ($\dot{d}$ =0) with k_{arm} set at 222 N/m.

$$F_d = k_{arm}\, d + c_{arm}\,\dot{d} \tag{5}$$

3 Simulation results and discussion

Fig. 3 shows the percentage of the gravitational torque provided by the exoskeleton in ideal alignment conditions between SJC and ExoJC throughout the exoskeleton working range, by assuming that the exoskeleton is worn by a 70 kg and 1.7 m user and that the MKM's supply pressure is 4.3 bar.

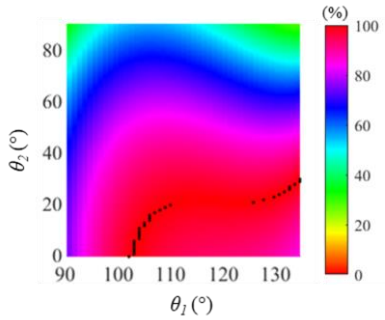

Fig.3 Percentage of torque support for ideal joints alignments. θ_1 and θ_2 are the shoulder and elbow flexion angles, respectively. Black dots highlight the working positions in which the gravitational and support torque are equal.

However, the precise location of SJC is unknown so a perfect alignment between ExoJC and SJC is hardly obtained wearing the exoskeleton. Therefore, the eight initial ExoJC positions illustrated in Fig. 4, plus the case in which a perfect alignment between ExoJC and SJC is supposed in the initial position (θ_1=90°), have been examined. All 8 ExoJC initial positions considered are 1 cm away from SJC.

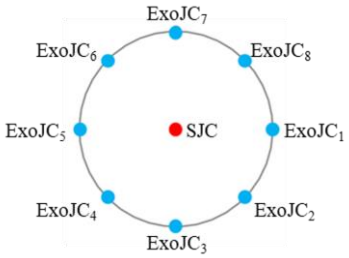

Fig.4 Maps of the ExoJC at starting position.

In addition to the initial offset, the physiological SJC displacement [9] during arm flexion must be taken into account to estimate Δy throughout the exoskeleton working range. The percentage of the gravitational torque provided by the exoskeleton in these scenarios is shown in Fig.5.

When the initial position of ExoJC coincides with SJC (Fig. 5e), the working range in which the support torque exceeds 80% is reduced compared to the ideal case (Fig. 3). At the same time, the workspace where the support torque is less than

60% also decreases. The initial offset between SJC and ExoJC further worsens the performance. Specifically, when the elbow and shoulder flexion angles are around 90°, the exoskeleton does not adequately support the user if ExoJC is over SJC (Fig. 5 g, h, i). The support torque in these situations is roughly twice the gravitational shoulder torque. Consequently, the wearer pushes down on the exoskeleton bracelet to prevent the upper arm elevation. As a result, an excessive increase in the activity of the shoulder extensor muscles would result from the reduction of the activity of flexor muscles.

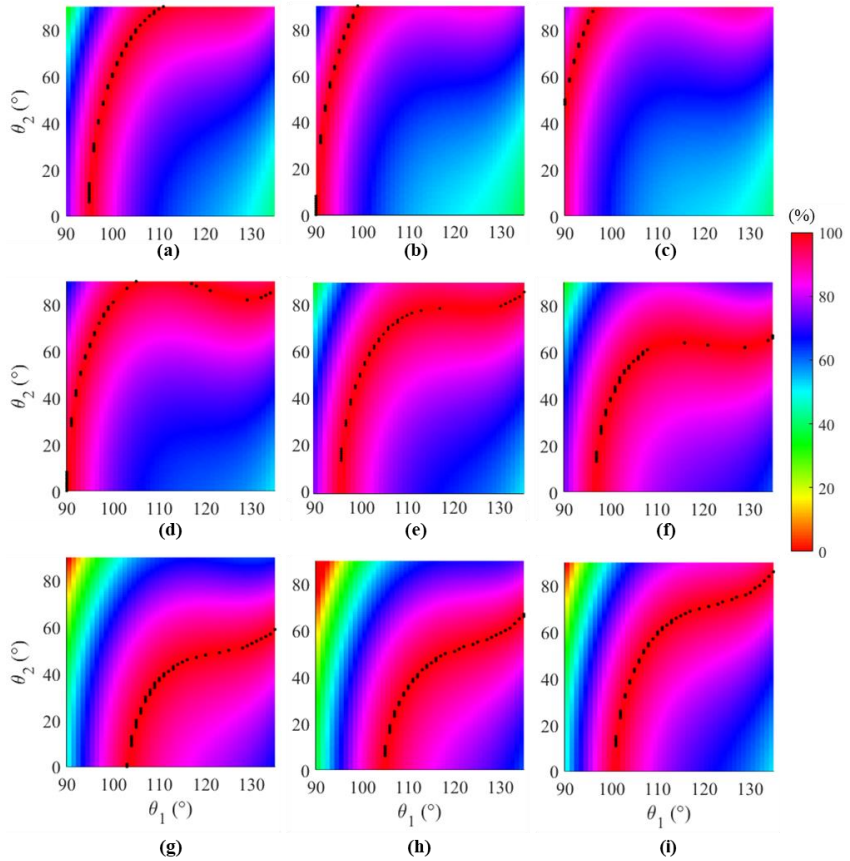

Fig.5 Percentages of torque support for different ExoJC positions: $ExoJC_1$ (a); $ExoJC_2$ (b); $ExoJC_3$ (c); $ExoJC_4$ (d); exact alignment in the initial position (e); $ExoJC_5$ (f); $ExoJC_6$ (g); $ExoJC_7$ (h); $ExoJC_8$ (i). θ_1 and θ_2 are the shoulder and elbow flexion angles, respectively. Black dots highlight the working positions in which the gravitational and support torque are equal.

With few notable exceptions, the exoskeleton generally compensates for misalignments rather effectively, and under typical operating conditions, the support torque exceeds 50%. Furthermore, it provides users with sufficient support without putting the user's arm under potentially harmful shear stress. The shear force applied to the arm (Fig. 6), in fact, does not increase to unreasonably high levels.

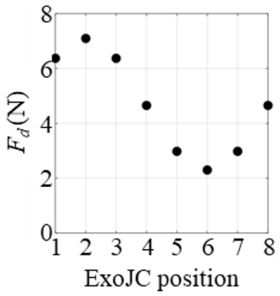

Fig.6 The estimated shear force magnitude for the different ExoJC positions illustrated in Fig. 4.

4 Conclusion

A kinematic chain with a limited number of degrees of freedom allows to design an exoskeleton with a compact and lightweight structure. At the same time, misalignments between the axes of rotation of the exoskeleton and those of the shoulder joint inevitably occur. These misalignments reduce the effectiveness of the exoskeleton and produce shear forces on the user's arm.

However, through simulations it was possible to demonstrate that, in a working range wide enough to carry out much of the work activities, an upper limb exoskeleton with just two degrees of freedom may provide a supporting torque of more than 50% of the shoulder gravitational load without introducing high contact forces on the user's arm that will cause discomfort in the user. In the future, simulations should be repeated for subjects with different anthropometric characteristics to consider intersubject variability, and the simulations' results should be validated by experimental trials.

References

1. Cui, X., Chen, W., Jin, X., Agrawal, S.K.: Design of a 7-DOF Cable-Driven Arm Exoskeleton (CAREX-7) and a Controller for Dexterous Motion Training or Assistance. IEEE/ASME Trans Mechatron 22, 161–172 (2017). https://doi.org/10.1109/TMECH.2016.2618888
2. Lo, H.S., Xie, S.Q.: Exoskeleton robots for upper-limb rehabilitation: State of the art and future prospects. Medical Engineering & Physics 34, 261–268 (2012). https://doi.org/10.1016/j.medengphy.2011.10.004
3. Hyun, D.J., Bae, K., Kim, K., Nam, S., Lee, D.: A light-weight passive upper arm assistive exoskeleton based on multi-linkage spring-energy dissipation mechanism for overhead

tasks. Robotics and Autonomous Systems 122, 103309 (2019). https://doi.org/10.1016/j.robot.2019.103309
4. Liu, C., Liang, H., Murata, Y., Li, P., Ueda, N., Matsuzawa, R., & Zhu, C.: A wearable lightweight exoskeleton with full degrees of freedom for upper-limb power assistance. Advanced Robotics, 35(7), 413–424 (2021). https://doi.org/10.1080/01691864.2020.1854115
5. Schiele, A., Van Der Helm, F.C.T.: Kinematic Design to Improve Ergonomics in Human Machine Interaction. IEEE Trans Neural Syst Rehabil Eng 14, 456–469 (2006). https://doi.org/10.1109/TNSRE.2006.881565
6. Pacifico, I., Scano, A., Guanziroli, E., Moise, M., Morelli, L., Chiavenna, A., Romo, D., Spada, S., Colombina, G., Molteni, F., Giovacchini, F., Vitiello, N., Crea, S.: An Experimental Evaluation of the Proto-MATE: A Novel Ergonomic Upper-Limb Exoskeleton to Reduce Workers' Physical Strain. IEEE Robot Automat Mag 27, 54–65 (2020). https://doi.org/10.1109/MRA.2019.2954105
7. Du, Z., Yan, Z., Huang, T., Bai, O., Huang, Q., Zhang, T., Han, B.: Development and Experimental Validation of a Passive Exoskeletal Vest. IEEE Transactions on Neural Systems and Rehabilitation Engineering, 30, 1941-1950 (2022). https://doi.org/10.1109/TNSRE.2022.3189666
8. Balser, F., Desai, R., Ekizoglou A., Bai, S.: A Novel Passive Shoulder Exoskeleton Designed With Variable Stiffness Mechanism. IEEE Robotics and Automation Letters, 7(2), 2748-2754 (2022). https://doi.org/10.1109/LRA.2022.3144529
9. Castro, M. N., Rasmussen, J., Andersen, M. S., Bai, S.: A compact 3-DOF shoulder mechanism constructed with scissors linkages for exoskeleton applications. Mechanism and Machine Theory, 132, 264-278 (2019). https://doi.org/10.1016/j.mechmachtheory.2018.11.007
10. Rossini M., De Bock, S., van der Have, A., Flynn, L., Rodriguez-Cianca D., De Pauw, K., Lefeber, D., Geeroms, J., Rodriguez-Guerrero, C.: Design and Evaluation of a Passive Cable-Driven Occupational Shoulder Exoskeleton. IEEE Transactions on Medical Robotics and Bionics. 3(4), 1020-1031 (2021). https://doi.org/10.1109/TMRB.2021.3110679
11. Maurice, P., Camernik, J., Gorjan, D., Schirrmeister, B., Bornmann, J., Tagliapietra, L., Latella, C., Pucci, D., Fritzsche, L., Ivaldi, S., Babic, J.: Objective and Subjective Effects of a Passive Exoskeleton on Overhead Work. IEEE Trans Neural Syst Rehabil Eng 28, 152–164 (2020). https://doi.org/10.1109/TNSRE.2019.2945368
12. Magnetti Gisolo, S., Muscolo, G.G., Paterna, M., De Benedictis, C., Ferraresi, C.: Feasibility Study of a Passive Pneumatic Exoskeleton for Upper Limbs Based on a McKibben Artificial Muscle. In: Zeghloul, S., Laribi, M.A., and Sandoval, J. (eds.) Advances in Service and Industrial Robotics. pp. 208–217. Springer International Publishing, Cham (2021). https://doi.org/10.1007/978-3-030-75259-0_23
13. Paterna, M., Magnetti Gisolo, S., De Benedictis, C., Muscolo, G.G., Ferraresi, C.: A passive upper-limb exoskeleton for industrial application based on pneumatic artificial muscles. Mech. Sci. 13, 387–398 (2022). https://doi.org/10.5194/ms-13-387-2022.
14. Nef, T., Riener, R.: Shoulder actuation mechanisms for arm rehabilitation exoskeletons. In: 2008 2nd IEEE RAS & EMBS International Conference on Biomedical Robotics and Biomechatronics. IEEE, Scottsdale, AZ, USA, 862–868 (2008). https://doi.org/10.1109/BIOROB.2008.4762794